International Journal of Engineering

Journal Homepage: www.ije.ir

Metallurgical and Mechanical Properties of Laser Cladded AlFeCuCrCoNi-WC_{10} High Entropy Alloy Coating

A. Vyas*[a], J. Menghani[a], H. Natu[b]

[a] *Mechanical Engineering Department, SVNIT, Surat, India*
[b] *Magod Fusion Technologies Private Limited, Pune, India*

PAPER INFO

Paper history:
Received 17 May 2020
Received in revised form 06 June 2020
Accepted 12 June 2020

Keywords:
Laser-assisted Cladding
Microhardness
High Entropy Alloy
Microstructure

ABSTRACT

In spite of excellent corrosion resistance, good ductility and low cost of AISI 316 austenitic stainless steel, the low hardness and poor mechanical characteristic of material restricts its applicability in several industrial services. To improve the mechanical properties AlFeCuCrCoNi-WC_{10} high-entropy alloy coatings were deposited via laser cladding on austenitic stainless steel AISI 316 substrate. The influence of WC on phase constituents, microstructure, microhardness and elemental distribution were investigated using X-ray diffractometry, optical microscopy microhardness tester and FESEM-EDS (Energy Dispersive Spectroscopy), respectively. The XRD peaks revealed that as clad AlFeCuCrCoNi-WC_{10} multiple principal element alloy coating composed of BCC, FCC and W-rich phase. The cladding zone microstructure is mainly consisting of fine-grained non-directional and equiaxed crystals away from the base material and columnar grains near the base material. The energy dispersive spectroscopy indicated segregation of W and Cr in the interdendritic region. However, other elements of the multiple principal element alloy are observed to be uniformly distributed throughout the cladding. The microhardness of the AlFeCuCrCoNi-WC_{10} (670 $Hv_{0.5}$) high entropy alloy coating was 4.5 times greater than that of substrate AISI-316.

***doi**: 10.5829/ije.2020.33.07a.27*

1. INTRODUCTION

In order to overcome the restrictions such as elemental segregation and formation of various brittle phases in the conventional alloying system, Yin et al. [1] discovered the innovative idea of multi principal element alloy (high entropy alloy). The high entropy alloy (baseless alloy, multi principal element) can be defined as solid solution alloys which have a minimum of five principal elements, but not greater than thirteen elements, each of the primary elements having a contribution in between 5 to 35 at% [1-2]. The baseless alloys have some excellent characteristic such as superior wear resistance, distinctive magnetic as well as electrical properties, better resistance to erosion, excellent stability at various temperature range, high hardness and mechanical strength due to its four core effect namely cocktail effect, severe lattice distortion effect, sluggish diffusion effect as well as high entropy effect [3]. However, bulk products of high entropy alloys are usually made of casting as well as powder metallurgy route. To improve efficiency and working life of various components along with reduced cost of high entropy alloy (Ni, Cr and Co expensive elements), it can be used as a coating material instead of replacement of existing bulk material [4]. The HEA coating is deposited through different processes such as plasma transferred arc, magneto sputtering, electrochemical deposition and laser coating. Laser is a versatile tool which can be used not only for cladding but also for welding, cutting as well as forming [5-8]. The laser-assisted coating method has many advantages compared to other methods, including rapid solidification rate (in the range of 10^4 to 10^6 $^oC/s$), good metallurgical bonding, optimum dilution, narrow heat-affected zone, better control on process parameters, high repeatability and process stability. In addition, based on

*Corresponding Author Email: *akku.vyas2011@gmail.com* (A. Vyas)

Please cite this article as: A. Vyas, J. Menghani, H. Natu, Metallurgical and Mechanical Properties of Laser Cladded AlFeCuCrCoNi-WC_{10} High Entropy Alloy Coating, International Journal of Engineering (IJE), IJE TRANSACTIONS A: Basics Vol. 33, No. 7, (July 2020) 1397-1402

kinetic theory, the reduction in nucleation growth of brittle intermetallics can be done through a quick solidification rate of the laser cladding process [9]. AISI 316 steel is a very important material for many tribological as well as marine applications due to its superior corrosive resistivity and ductility. However, its inferior tribological and wear characteristics impose a limitation on this material for a broader range of applications [10]. From the theoretical point of view and practical consideration, it is necessary to investigate the mechanical and metallurgical characteristics of HEA cladding on austenitic steel in brief. Recently, ceramic particles such as WC, TiC and SiC reinforced coatings prepared by laser cladding technology are mostly applied on Nickel, Cobalt or Ferrous alloys. However, the investigation regarding HEA coating strengthened by reinforcing phase particles are limited. WC has very high hardness (2600 HV) and melting point (2600 ^{o}C) making it ideal as a reinforcement material in HEA coating to enhance mechanical characteristics [11,16]. In present work, a novel high entropy alloy coating with an equiatomic composition of AlFeCuCrCoNi- and 10 wt.% WC (AlFeCuCrCoNi-WC_{10}) was deposited on AISI-316 substrate through laser cladding. Furthermore, the phase constituents, microstructure evaluation, elemental distribution and microhardness of high entropy alloy coating were investigated briefly.

2. EXPERIMENTAL PROCEDURE

Circular samples of AISI 316 stainless steel with a size of ϕ90mm x 10mm were chosen as the base material. The elemental composition of AISI 316 steel is as indicated in Table 1. As a cladding material, an equiatomic Fe, Cr, Co, Ni, Cu and Al metal powders with a reinforcement of 10 wt.% WC were used. The contribution of individual elements for making high entropy alloy is as listed in Table 2. The motive behind selecting a particular individual element for the preparation of high entropy alloy is mixing enthalpy of every principal element with each other, as listed in Table 3 [16].

All powders having 99.9% purity procured from Chrome special materials pvt ltd., Mumbai with an average mesh size of 80-100 were used in the present investigation. The substrate surface was polished through emery paper (320-1200 grit size) and rinsed with the acetone before laser cladding. The selected high entropy alloy powders (AlFeCuCrCoNi-WC_{10}) were mixed in an equiatomic composition using 3D Multi-Motion Mixer (Alphie 0.3 Hp) for 30 minutes (15 min forward and 15 min reverse cycle). The laser cladding experiment was performed through 4 kW CO_2 laser system situated at the Magod Fusion Technology, Pune, as shown in Figure 1. The operating parameters for laser cladding process were, spot diameter (d) = 2.4 mm, standoff distance (a) = 8 mm, laser power (p) = 1.1 kW, laser scanning velocity (v) = 500 mm/min, argon flow rate (r) = 6 lit/min and the powder feed rate (f) = 4 g/min. An overlapping ratio of 60% was chosen between successive tracks to generate a homogeneous cladding on the substrate. The laser cladded metallurgical specimens were cut cross-sectional, resin mounted, polished, and etched with an aqua regia solution. The difference in clad morphology and

TABLE 1. Chemical content of AISI 316 steel (wt.%).

Elements	Ni	Mo	P	S	N_2	C	Mg	Si	Cr	Fe
Composition	10.0 - 14.0	2.00 - 3.00	0.045	0.03	0.1	0.08	2.00	0.1	16.0 -18.0.	65-70

TABLE 2. Chemical composition of AlFeCuCrCoNi-WC_{10} high entropy alloy powder (wt.%).

Elements	Al	Fe	Cu	Co	Cr	Ni	WC
Composition	7.96± 0.40	15.90± 0.10	17.73± 0.05	16.52± 0.20	14.68± 0.05	17.14± 0.25	10.00 ± 0.05

TABLE 3. Binary mixing enthalpies, $\Delta H^{mix}ij$ (kJ/mol) of high entropy alloy [16]

Al-Fe	-11	Fe-Ni	2	Cu-Ni	4	Cr-Ni	-7	Co-Ni	0	Ni-W	-9
Al-Ni	-22	Fe-Cu	13	Cu-Co	6	Cr-Co	-4	Co-W	-5	Ni-C	-39
Al-Cu	-1	Fe-Co	-1	Cu-Cr	12	Cr-W	5	Co-C	-42		
Al-Co	-19	Fe-Cr	-1	Cu-W	23	Cr-C	-61				
Al-Cr	-10	Fe-W	4	Cu-C	-42						
Al-W	-2	Fe-C	-50								
Al-C	-30										

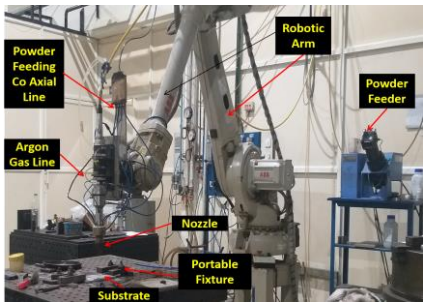

Figure 1. A 4 kW Co_2 laser cladding experimental setup equiped with robotic arm

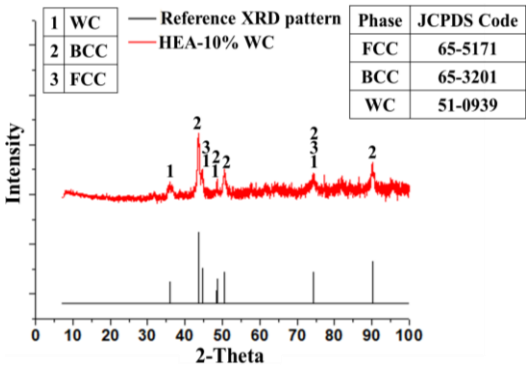

Figure 2. XRD spectra of AlFeCuCrCoNi-WC_{10} HEA

microstructure along its length and height was revealed by optical microscopy (Leica S8APO). The phase constitution of the as cladded specimen was identified through X-ray diffractometer (XRD) using a Cu Kα radiation (PANalytical X'Pert Powder). The variation in microhardness from cladded zone to substrate metal was determined using a Micro Vickers Hardness Tester (Future Tech Corporation, Japan –FM 700) applying a load of 0.5 Kg with a dwell time of 15 Sec. The field emission scanning electron microscope (FESEM-JSM7100F) along with energy dispersive spectrometer (EDS) was used to analyze the elemental distribution in the coating as well as in the interface zone.

3. RESULTS AND DISCUSSION

3. 1. Phase Constituents Figure 2 indicates the X-ray diffraction profile of the AlFeCuCrCoNi-WC_{10} high entropy alloy coating. The solid solution phases consisting of a combination of two phases FCC + BCC, an additional set of diffraction peaks corresponding to W rich carbide phases can be observed [12]. The results revealed that additional phases in the coating observed to be very limited and the laser rapid melting and solidification process effectively constrained the precipitation of undesired intermetallic compounds in the cladding. No oxide formation was revealed in XRD Spectra, which signifies that during laser cladding adequate protection against oxidation was maintained through continuous supply of Argon gas [13]. As stated by Gibbs phase rule, the number of phases for non-equilibrium solidification leads to be $p > n+1$ (p= number of phases, n= number of elements), while the phases formed in AlFeCuCrCoNi-WC_{10} high entropy alloy cladding is much less than 8 [14]. The reason behind this phenomenon is the influence of high mixing entropy generated by multi principal element. Considering intensity of XRD peaks, it is observed that BCC solid solution phase is much higher than that of FCC solid solution phase, and it can be concluded that the BCC solid solution phase is the primary phase [15].

3. 2. Microstructure Figure 3 shows the optical micrograph of AlFeCuCrCoNi-WC_{10} HEA coatings synthesized through the laser-assisted cladding. The micrograph indicates that cladding is dense enough and free from cracks as well as pores, with a coating thickness of 0.9 mm. As can be seen in Figure 3(a), there are three categorical regions in the cladding, that is clad zone (CZ), Bonding Zone (BZ) and Heat affected zone (HAZ) the span of which depends on variation in the microstructure. The cladding zone microstructure is mainly consisting of fine-grained non-directional and equiaxed crystals away from the base material and columnar grains near the base material. The columnar grains (Figure 3(c)) are transformed to equiaxed (Figure 3(b)) with a reduction in a temperature gradient in the center of the cladding zone. The layer of planar crystals with a thickness of approximately 20-25 μm is observed at the interface region of the high entropy alloy cladding, as indicated by "PC" in Figure 3 (a). The planar crystal is hard to corrode for metallurgical investigation. In addition, the curved line at the interface zone instead of a straight line also indicates an excellent metallurgical bonding between the cladding and the base material. When the high entropy alloy cools down during laser cladding process, agreeing to the constitutional undercooling criterion, the temperature difference at liquid solid interface and the cooling rate are the major factors to identify the microstructure behavior of HEA. In the laser cladding process, due to quick melting-solidification phenomena a thin layer of substrate melts with the cladding layer, and this diffused layer cools down through heat dissipation of the base material. Therefore, the temperature difference (Δt) is very high, while the solidification rate (r) is less, which tends to give large Δt/r. Therefore, the nucleation rate is much quicker than the growth rate of the crystal and it will lead to grow as the planar crystal at the interface [16-18]. The growth direction of the columnar grain is perpendicular to the interface zone due to the rapid directional solidification, typical of the laser cladding process [19].

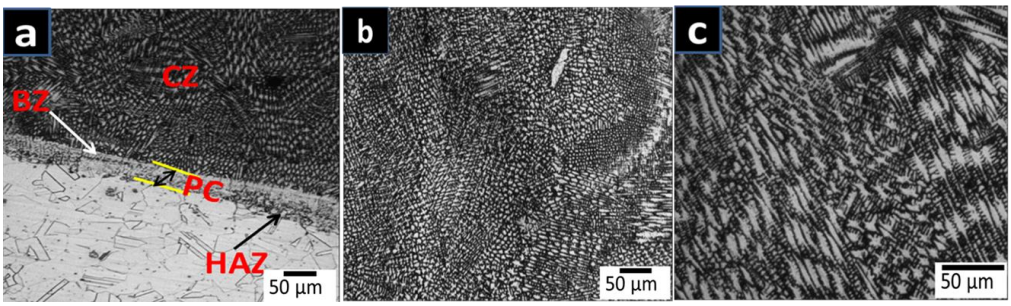

Figure 3. Optical micrograph of the HEA coatings (a) Interface zone (b) Cladding zone and (c) Grain orientation near the interface zone

3. 3. Compositional Analysis The EDS (Energy Dispersive Spectroscopy) results (Figure 4(b)) for the elemental composition of the cladding layer revealed that all the individual principal element were uniformly distributed in approximately designed weight proportion across the coating. The quantitative composition of elements in the different areas as indicated in region 1 (Bright) and region 2 (Dark) in Figure 4(c) is shown in Table 5. The elemental distribution in the region 2 (Dendritic) is similar to the quantitative composition of the cladding, while region 1 (Interdendritic) is enriched with tungsten particles. [18]. Additionally, high proportion of Cr is observed in interdendritic region indicating partial dissolution of tungsten carbide particles and replacement of W with Cr. This could be majorly due to the capillary phenomena of melted material and concentrated laser energy, which may tend to increase in the temperature of the molten pool beyond the melting point of tungsten carbide particles and lead to the partial dissolution of tungsten carbide particles [16].

Figure 5 shows the EDS elemental mapping for the individual elements in the cladding layer. As in area EDS analysis mapping also revealed the segregation of tungsten rich particles in the inter-dendritic region, while the other elements of the HEA are observed to be uniformly distributed throughout the cladding. The rapid melting and solidification process of laser cladding along with the sluggish diffusion effect of HEA leads to the uniform distribution of alloying elements [20]. In order to study the degree of iron dilution and its effect on the elemental distribution of the cladding layer, line EDS analysis was conducted near the interface zone, and the results are indicated in Figure 6. The concentration of the iron is higher than design composition at the interface as compared to surface due to dilution from iron based substrate.

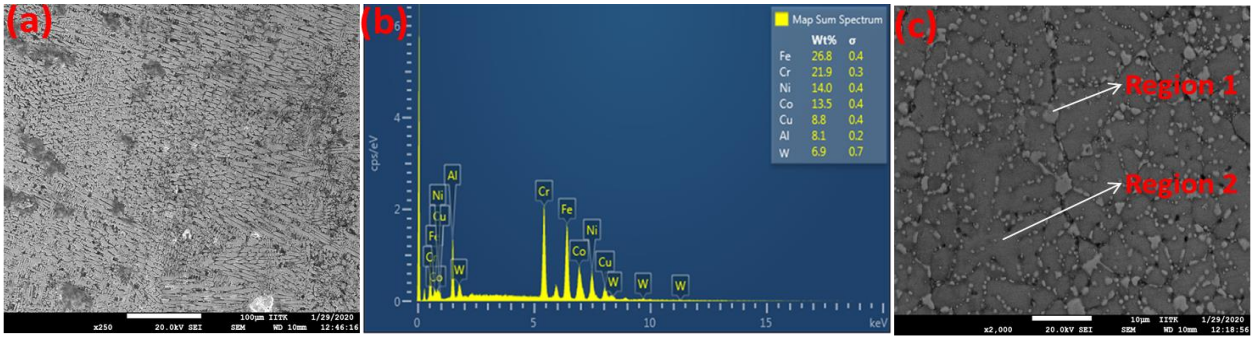

Figure 4. EDS elemental analysis of high entropy alloy coatings (a) SEM image of cladding zone (b) Elemental distribution of the cladding zone (c) High magnification image of cladding zone indicating various regions

TABLE 5.EDS results of AlFeCuCrCuNi-WC_{10} coating

Region	Fe	Cu	Cr	Co	Ni	Al	W
Region 1	14.6	8.3	26.1	7.4	8.8	3.6	31.2
Region 2	29.1	9.5	19.2	15.2	15.3	5.1	6.6

3. 4. Microhardness Figure 7 shows the measured values of microhardness for the AlFeCuCrCoNi-WC_{10} high entropy alloy coatings along the cross-section from the cladding zone to the substrate. It was observed that the maximum

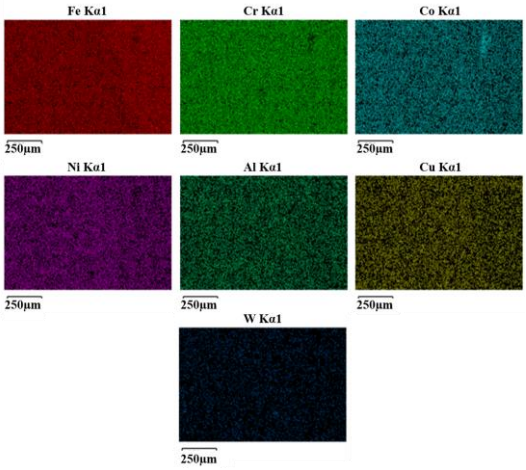

Figure 5. EDS maps of the HEA coating for elements Fe, Cr, Co, Ni, Al, Cu and W

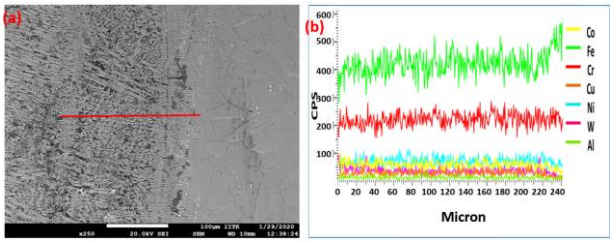

Figure 6. The line scan analysis of the AlFeCuCrCuNi-WC_{10} HEA coating (a) SEM micrograph of the interface zone of (b) Elemental distribution through line scan analysis

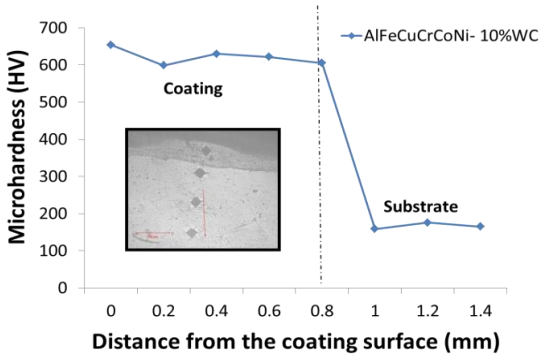

Figure 7. Microhardness distribution of the AlFeCuCrCoNi-WC_{10} coating

microhardness of AlFeCuCrCoNi-WC_{10} high entropy alloy coating reaches to 670 $HV_{0.5}$, which is approximately 4.5 times greater than the base material AISI-316 (155 $Hv_{0.5}$). This increasing hardness is attributed to the following reasons, (1) The ex-situ WC particles in the alloy coatings act as strengthening phase distributed in the solid solution phase due to the detachment of free carbon atoms from molten tungsten carbide particles into high entropy alloy matrix, increase lattice distortion and enhance solution strengthening. The substitutional and interstitial solution strengthening is the major phenomenon behind the solution strengthening of high entropy alloy. (2) The quick melting solidification behavior of the laser-assisted cladding process leads to grain size reduction, the development of nano-precipitates and the enhancement of solubility constrained in the coating. (3) The solution strengthening due to lattice distortion as a result of the difference in the atomic radius of the various metallic elements leads to large lattice strain distortion and solid solution effect in the AlCrFeNiCuCo-WC_{10} coatings. In addition, a high-density dislocation can be seen due to this variation in the atomic size. In AlCrFeNiCuCo-WC_{10}, Al contributes more to the lattice distortion because of its larger atomic radius compared to the other five elements. (4) Rapid solidification restricting grain growth leads to increasing the amount of grain boundary and tends to generate grain boundary strengthening [19].

4. CONCLUSION

The XRD peaks revealed that as clad AlFeCuCrCoNi-WC_{10} high entropy alloy coating composed of BCC, FCC and W-rich phase. The morphology of laser cladded AlFeCuCrCoNi-WC_{10} high entropy alloy includes cladding, bonding, planer crystal and heat-affected zones. The cladding zone microstructure is mainly consisting of fine-grained non-directional and equiaxed crystals away from the base material and columnar grains near the base material. The energy dispersive spectroscopy results revealed the segregation of W and Cr particles in the inter-dendritic region. At the same time, the other elements of the HEA are observed to be uniformly distributed throughout the cladding. The contribution of the iron is higher than that of the other elements near the substrate as compared to the cladding zone due to the rich iron content in the AISI-316substrate. Maximum microhardness of AlFeCuCrCoNi-WC_{10} high entropy alloy coating reaches 670 $HV_{0.5}$, which is approximately 4.5 times greater than that of the base material AISI-316 (155 $Hv_{0.5}$).

5. ACKNOWLEDGEMENT

The author appreciates the funding provided by the department of science and technology, India (DST-EMR/2016/000451) and ACMS department of IIT-Kanpur for metallurgical characterization.

6. REFERENCES

1. Yin, Shuo, Wenya Li, Bo Song, Xingchen Yan, Min Kuang, Yaxin Xu, Kui Wen, and Rocco Lupoi. "Deposition of FeCoNiCrMn high entropy alloy (HEA) coating via cold spraying." ***Journal of Materials Science & Technology,*** Vol. 35, No. 6, (2019), 1003-1007. doi: 10.1016/j.jmst.2018.12.015
2. Wall, Michael T., Mangesh V. Pantawane, Sameehan Joshi, Faith Gantz, Nathan A. Ley, Rob Mayer, Andy Spires, Marcus L. Young, and Narendra Dahotre. "Laser-coated CoFeNiCrAlTi high entropy alloy onto a H13 steel die head." ***Surface and Coatings Technology,*** Vol. 387 (2020), 125473. doi: 10.1016/j.surfcoat.2020.125473
3. Zhang, H. X., J. J. Dai, C. X. Sun, and S. Y. Li. "Microstructure and wear resistance of TiAlNiSiV high-entropy laser cladding coating on Ti-6Al-4V." ***Journal of Materials Processing Technology,*** (2020), 116671. doi: 10.1016/j.jmatprotec.2020.116671
4. Guo, Yaxiong, Huilin Wang, and Qibin Liu. "Microstructure evolution and strengthening mechanism of laser-cladding MoFexCrTiWAlNby refractory high-entropy alloy coatings." ***Journal of Alloys and Compounds,*** (2020), 155147. doi: 10.1016/j.jallcom.2020.155147
5. Safari, Mehdi, and Mahmoud Farzin. "Experimental investigation of laser forming of a saddle shape with spiral irradiating scheme." ***Optics & Laser Technology,*** Vol. 66, (2015), 146-150. doi: 10.1016/j.optlastec.2014.09.003
6. Safari, Mehdi, Hosein Mostaan, and Mahmoud Farzin. "Laser bending of tailor machined blanks: Effect of start point of scan path and irradiation direction relation to step of the blank." ***Alexandria Engineering Journal,*** Vol. 55, No. 2, (2016), 1587-1594. doi: 10.1016/j.aej.2016.01.010
7. Safari, Mehdi, and Hosein Mostaan. "Experimental and numerical investigation of laser forming of cylindrical surfaces with arbitrary radius of curvature." ***Alexandria Engineering Journal,*** Vol. 55, No. 3, (2016), 1941-1949. doi: 10.1016/j.aej.2016.07.033
8. Safari, M., M. Farzin, and H. Mostaan. "A novel method for laser forming of two-step bending of a dome shaped part." ***Iranian Journal of Materials Forming*** Vol. 4, No. 2, (2017), 1-14. doi: 10.22099/IJMF.2017.4288
9. Zhang, Hui, Ye Pan, Yizhu He, and Huisheng Jiao. "Microstructure and properties of 6FeNiCoSiCrAlTi high-entropy alloy coating prepared by laser cladding." ***Applied Surface Science,*** Vol. 257, No. 6, (2011), 2259-2263. doi: 10.1016/j.apsusc.2010.09.084
10. Khatak, H_S, and Baldev Raj, eds. Corrosion of austenitic stainless steels: mechanism, mitigation and monitoring. ***Woodhead Publishing***, 2002.
11. Jabbar Hassan, A., T. Boukharouba, D. Miroud, and S. Ramtani. "Metallurgical and Mechanical Behavior of AISI 316-AISI 304 during Friction Welding Process." ***International Journal of Engineering, Transactions B: Applications,*** Vol. 32, No. 2 (2019), 306-312. doi: 10.5829/ije.2019.32.02b.16
12. Desale, Girish R., C. P. Paul, B. K. Gandhi, and S. C. Jain. "Erosion wear behavior of laser clad surfaces of low carbon austenitic steel." ***Wear,*** Vol. 266, No. 9-10 (2009), 975-987. doi: 10.1016/j.wear.2008.12.043
13. Gu, Zhen, Shengqi Xi, and Chongfeng Sun. "Microstructure and properties of laser cladding and $CoCr_{2.5}FeNi_2Ti_x$ high-entropy alloy composite coatings." ***Journal of Alloys and Compounds,*** Vol. 819, (2020), 152986. doi: 10.1016/j.jallcom.2019.152986
14. Fang, Shoushi, Xueshan Xiao, Lei Xia, Weihuo Li, and Yuanda Dong. "Relationship between the widths of supercooled liquid regions and bond parameters of Mg-based bulk metallic glasses." ***Journal of Non-Crystalline Solids,*** Vol.321, No. 1-2 (2003), 120-125. doi:10.1016/S0022-3093(03)00155-8
15. Singh, Sheela, Nelia Wanderka, B. S. Murty, Uwe Glatzel, and John Banhart. "Decomposition in multi-component AlCoCrCuFeNi high-entropy alloy." ***Acta Materialia,*** Vol.59, No. 1 (2011), 182-190. doi: 10.1016/j.actamat.2010.09.023
16. Peng, Y. B., W. Zhang, T. C. Li, M. Y. Zhang, L. Wang, Y. Song, S. H. Hu, and Y. Hu. "Microstructures and mechanical properties of FeCoCrNi high entropy alloy/WC reinforcing particles composite coatings prepared by laser cladding and plasma cladding." ***International Journal of Refractory Metals and Hard Materials,*** Vol. 84 (2019), 105044. doi: 10.1016/j.ijrmhm.2019.105044
17. Kuldeep, B., K. P. Ravikumar, and S. Pradeep. "Effect of Hexagonal Boron Nitrate on Microstructure and Mechanical Behavior of Al7075 Metal Matrix Composite Producing by Stir Casting Technique." ***International Journal of Engineering, Transactions A: Basics,*** Vol. 32, No. 7 (2019), 1017-1022. doi: 10.5829/IJE.2019.32.07A.15
18. Khajesarvi, A., and G. Akbari. "Effect of Mo addition on nanostructured Ni50Al50 intermetallic compound synthesized by mechanical alloying." ***International Journal of Engineering-Transection C: Aspects,*** Vol. 28 (2015), 1328. doi: 10.5829/idosi.ije.2015.28.09c.10
19. Wen, Xin, Xiufang Cui, Guo Jin, Xuerun Zhang, Ye Zhang, Dan Zhang, and Yongchao Fang. "Design and characterization of FeCrCoAlMn0. 5Mo0. 1 high-entropy alloy coating by ultrasonic assisted laser cladding." ***Journal of Alloys and Compounds,*** (2020), 155449. doi: 10.1016/j.jallcom.2020.155449
20. Qiu, Xing-wu. "Corrosion behavior of $Al_2CrFeCo_xCuNiTi$ high-entropy alloy coating in alkaline solution and salt solution." ***Results in Physics,*** Vol.12 (2019), 1737-1741. doi: 10.1016/j.rinp.2019.01.090

Persian Abstract

چکیده

علی‌رغم مقاومت در برابر خوردگی عالی، شکل‌پذیری خوب و هزینه‌ی پایین فولاد زنگ‌نزن آستنیتی AISI 316، به علت سختی کم و ویژگی‌های مکانیکی ضعیف، کاربرد آن در چند زمینه‌ی صنعتی محدود می‌شود. برای بهبود ویژگی‌های مکانیکی، پوشش‌های آلیاژی آنتروپی بالای AlFeCuCrCoNi-WC10 از طریق روکش‌کاری فلزی با استفاده از لیزر بر روی زیرلایه‌ی فولاد زنگ‌نزن آستنیتی AISI 316 قرار گرفتند. تاثیر ترکیب WC بر ترکیب دیگر فازها، ریزساختار، ریزسختی و توزیع عناصر به‌ترتیب با طیف‌نگار پرتو ایکس، طیف‌سنجی پراکندگی انرژی (FESEM-EDS) آزمایش‌گر میکرو سختی بررسی شد. قله‌های XRD نشان داد که به سطح پوشیده‌شده با AlFeCuCrCoNi-WC10 ، حاوی فاز غنی از W با ساختار BCC و FCC است ریزساختار ناحیه‌ی پوششی عمدتاً از بلورهای ریزدانه‌ی غیرجهت‌دار و مخلوط در نواحی دور از مواد پایه، و دانه‌های ستونی در نزدیکی مواد پایه تشکیل شده است. طیف‌سنجی پراکندگی انرژی، تفکیک W و Cr را در منطقه‌ی فصل مشترک نشان داد. البته، آن طورکه مشاهده شد، سایر عناصر آلیاژی به‌طور یک‌نواخت در سراسر روکش توزیع شده‌اند. ریزسختی پوشش آلیاژی آنتروپی بالا (AlFeCuCrCoNi-WC10) ۶۷۰ عدد ریزسختی ویکرز ۰/۵ (670 Hv0.5)، یعنی ٤/٥ برابر بیشتر از ماده‌ی زیرلایه (AISI-316) بود.